Journal of Thermal Analysis and Calorimetry
https://doi.org/10.1007/s10973-025-14204-w

Combustion characteristics and efficiency of raw and clean lignite samples by thermal analysis techniques: TG–DTG–MID, DSC, and PDSC applications

Mustafa Versan Kök[1,5] · **Georg Matuschek**[2] · **Mikhail A. Varfolomeev**[3] · **Danis K. Nurgaliev**[4]

Received: 26 February 2024 / Accepted: 10 March 2025

Abstract

This study investigates the combustion characteristics and efficiency of six distinct lignite samples, comparing their untreated and treated forms. The experimental approach employs simultaneous thermogravimetry coupled with multiple ion detection (TG–DTG–MID) as well as differential and pressurized scanning calorimetry (DSC–PDSC) techniques. This integrated methodology provides a thorough understanding of the combustion mechanisms involved. The experiments are conducted under a controlled heating rate of 10 °C min^{-1} across a broad temperature range of 25 to 650 °C. Additionally, PDSC assessments are performed under varying pressure conditions, ranging from 100 to 300 psig, while maintaining the same heating rate. Distinct reaction phases such as evaporation, primary carbonization, and mineral matter decomposition are identified through detailed analyses of the untreated and treated lignite samples. Key combustibility indices, including reactivity and the ignition–combustion index, are systematically evaluated for both untreated and treated specimens. These metrics offer valuable insights into the combustion behavior and efficiency of the lignite samples under different treatment conditions.

Keywords Lignite · Coal · Combustion · Thermogravimetry · Mass spectrophotometry · Differential scanning calorimeter · Pressure

List of symbols

R_{max}	Maximum combustion rate
R_a	Average mass loss rate
W_o	Initial mass of the sample
dW/dt	Maximum rate of mass loss
T_i	Ignition temperature
T_b	Burnout temperature
t_m	Time which corresponds to the maximum combustion rate
t_i	Ignition time which corresponds to ignition temperature

Introduction

Over the past two decades, there has been a growing focus on the use of thermal analysis methods to study various fossil fuels, including coal, lignite, crude oil, oil shale, and asphaltites. Among these, lignite holds particular significance as a primary energy source in Türkiye, widely used in power generation and domestic heating. Consequently, reducing ash and sulfur content through washing processes has become essential to produce a more environmentally friendly fuel. Thermoanalytical techniques, such as thermogravimetry (TG–DTG), differential thermal analysis (DTA), differential scanning calorimetry (DSC), and mass spectrometry (MS), play a crucial role in this effort, providing a detailed understanding of the thermal properties of fossil fuels. These include parameters

✉ Mustafa Versan Kök
kok@metu.edu.tr

[1] Petroleum and Natural Gas Engineering Department, Middle East Technical University, Inonu Bulvari, 06531 Ankara, Turkey

[2] Comprehensive Molecular Analytics, Department of Environmental Sciences, Helmholtz-Center Munich - German Research Center for Environmental Health, Munich, Germany

[3] Department of Physical Chemistry, Kazan Federal University, Kremlevskaya str. 18, 420008 Kazan, Russia

[4] Institute of Geology and Petroleum Technologies, Kazan Federal University, Kremlevskaya str. 18, 420008 Kazan, Russia

[5] Turkish - Japanese Science and Technology University, Teknopark Bulvarı, No: 1/11C Kat: 4, 34906 Pendik, İstanbul, Turkey

such as peak temperature, burnout temperature, mass loss, combustion profiles, and pressure dynamics.

Numerous studies have investigated the combustion characteristics and reaction kinetics of coal samples across different ranks. Comparative analyses have evaluated a range of parameters, including peak temperature, burnout temperature, moisture content, ash content, volatile matter, fixed carbon, and calorific value [1–4]. Research has also explored the combustion profiles of coal samples under varying heating rates, highlighting their influence on peak and burnout temperatures. Additionally, investigations into the pyrolysis and combustion behavior of coals with different ranks and maceral compositions have considered factors such as particle size, using techniques like TG–DTG [5–7].

Findings from these studies reveal consistent trends, such as lower initiation temperatures for lower-ranked coals and convergence of thermal behavior among coals with similar vitrinite content [8–11]. Kinetic models, including model-free methods, are commonly employed to analyze kinetic data at different heating rates. Parameters such as activation energy and Arrhenius constants are frequently calculated and discussed to provide deeper insights into coal combustion processes [12–15].

Aligned with this research trajectory, the present study examines the combustion characteristics and efficiency of six distinct lignite samples from the Thrace Basin in Türkiye, in both their raw and washed states. The methodologies employed include thermogravimetry coupled with multiple ion detection (TG–DTG–MID), differential scanning calorimetry (DSC), and pressurized differential scanning calorimetry (PDSC).

Comparative analyses focus on various properties of the lignite samples, such as reaction zones, mass loss, and peak and burnout temperatures. The aim is to assess differences in combustion behavior, efficiency, intensity, and reactivity across the samples. This study provides valuable insights into the thermal dynamics of combustion processes, contributing to a more comprehensive understanding of lignite combustion kinetics in both raw and cleaned forms.

Experimental

Six lignite samples with diverse characteristics were selected from the Thrace region for experimental purposes and coded according to their properties and locations. These samples were processed in compliance with ASTM Standards (D 2013-72). Ash reduction (cleaning) procedures were applied to the processed samples. During this process, the lignite samples were crushed under controlled conditions using a jaw crusher, and their washability characteristics were evaluated through sink–float tests conducted at densities of 1.40, 1.50, 1.60, 1.70, and 1.80 g cm^{-3}. Zinc chloride was employed as the medium to mitigate the adverse effects of viscosity.

To prepare clean lignite feedstock for thermogravimetric and calorimetric analyses (TG–DTG and DSC experiments), the lignite samples were washed at specific densities. The optimal separation density for each fraction was identified based on the degree of washability, with the density providing the highest degree of washability selected as the optimum separation density. The final experimental products were prepared by blending the clean lignite obtained at these optimal densities and weighted according to their respective mass percentages [16].

The experimental framework included thermogravimetric analysis coupled with multiple ion detection (TG–DTG–MID), differential scanning calorimetry (DSC), and pressurized differential scanning calorimetry (PDSC). Controlled heating rates of 10 °C min^{-1} were applied over a broad temperature range of 25–650 °C. PDSC experiments were conducted at pressures ranging from 100 to 300 psig using the same heating rate. Approximately 10 mg of each lignite sample was used per experiment, with a constant airflow rate of 50 mL min^{-1} through the sample pan. It was assumed that the temperature distribution effects within the small-sized particles were negligible.

Prior to the experiments, meticulous calibrations of the thermal analysis systems for balance and temperature were performed. To ensure reliability and reproducibility, all experiments were conducted twice. The reproducibility of the results was acceptable, and the reported experimental error was consistently maintained at less than ± 0.5%.

Results and discussion

In thermal analysis, key parameters such as temperature, fuel composition, and oxygen availability play critical roles in determining the reaction dynamics during the interaction of oxygen with a given sample.

General geology

The Thrace region is of significant geological importance in Türkiye due to its extensive coal and hydrocarbon resources. This importance has driven numerous geological studies aimed at understanding the region's stratigraphy, tectonics, and resource potential. Coal formations within the Thrace Tertiary are primarily associated with the Danışmen Formation, historically considered to be of lower Miocene. The lignite deposits in the northern part of the Thrace Basin are predominantly located near the base of the Istranca Massif (Fig. 1). Key fields include Edirköy, Küçükyoncalı, Safaalan, Vize, Pınarhisar, and Demirhanlı [17, 18]. The geological settings of these deposits suggest a complex interplay of tectonic uplift and sedimentary processes, which have influenced both the distribution and quality of the lignite seams.

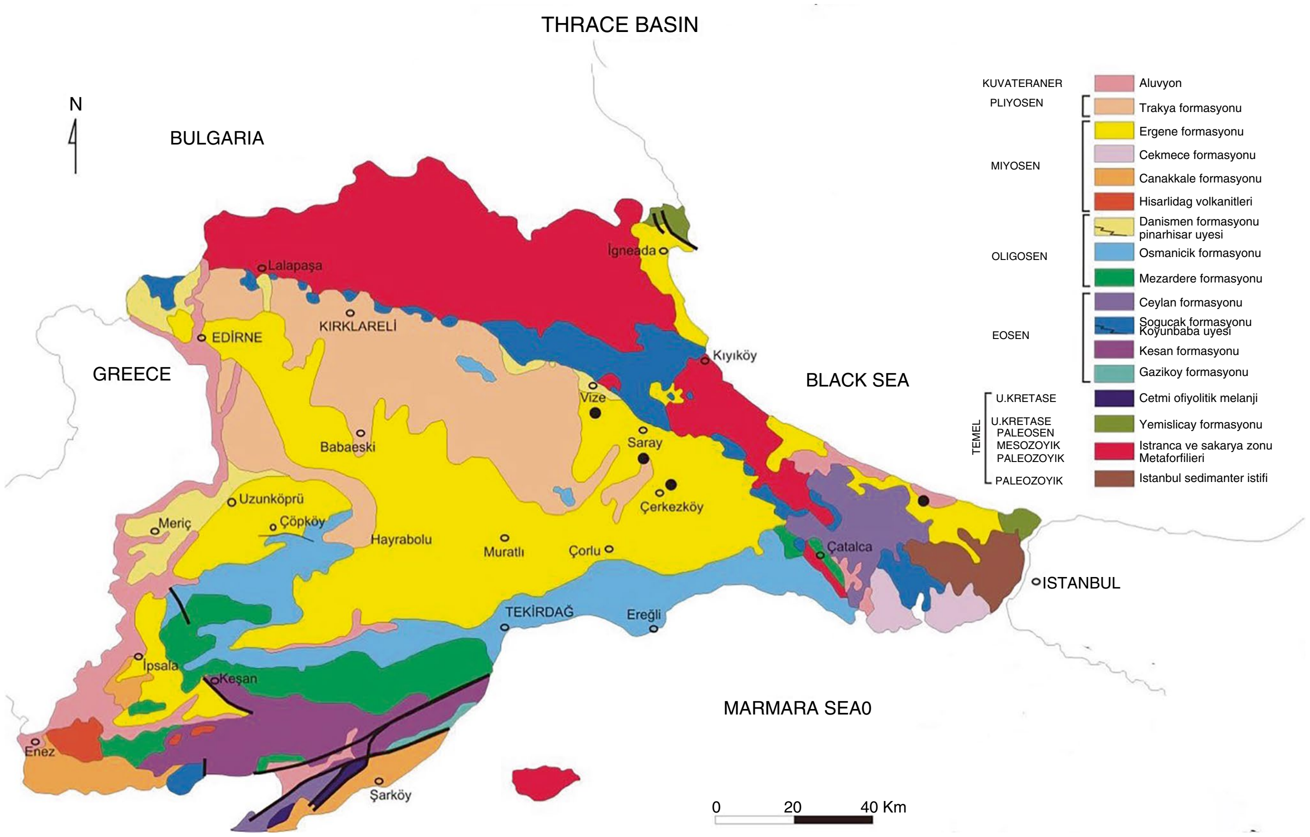

Fig. 1 Geological map of Thrace Basin [17]

Understanding these geological dynamics is crucial for optimizing the exploration and exploitation of these resources.

Properties of lignite samples

The properties of the lignite samples from the Thrace Basin were meticulously analyzed to determine their suitability for various applications, particularly in energy production. The raw lignite samples displayed heating values ranging from 2115 to 2395 kcal kg^{-1}, indicating a medium to low calorific value typical of lignite (Table 1). These values are suitable for domestic energy use but highlight the need for beneficiation processes to improve fuel quality for industrial applications. Vitrinite reflectance (R_{max}), a key indicator of coal rank, ranged from 0.433 to 0.502%, placing these samples in the lignite to sub-bituminous coal category. This range reflects the relatively low degree of coalification, consistent with the geological age and depositional environment of the Thrace Basin lignites. Detailed maceral analysis (Table 2) revealed that the lignites are predominantly composed of huminite, with contents ranging between 55 and 76%. This high huminite content suggests a peat-forming environment rich in organic material. Liptinite content, associated with hydrogen-rich components, ranged from 3 to 7%, while inertinite, indicative of oxidized or degraded organic material, ranged from 3 to 4%. The low inertinite content points to minimal oxidation during peat deposition, aligning with the humid and anoxic conditions inferred for the basin's paleoenvironment. The mineral matter content of the samples varied widely, between 9 and 32%. This variation is significant because mineral content directly impacts ash formation during combustion. Lignite with higher mineral content requires extensive cleaning to reduce ash production, which is critical for meeting environmental standards and improving combustion efficiency. The heterogeneity in mineral matter distribution also suggests varying depositional and diagenetic conditions across the sampled fields.

Scanning electron microscopy (SEM) analysis

Scanning electron microscopy (SEM) was utilized to examine the surface topography of raw and cleaned lignite samples, with high-resolution micrographs captured at magnifications of × 50 and × 1500 for samples 1, 2, and 3 (Fig. 2). These images illustrate the morphological differences between the raw and cleaned samples, providing insight into the effects of the cleaning process on particulate distribution and surface structure.

The SEM images of raw lignite samples reveal a predominance of fine and ultra-fine particulates distributed across the surface of coarser particles. These particulates often appear as dense clusters clogging the interstitial voids between larger

Fig. 2 SEM analysis of raw and clean lignite samples 1, 2, and 3

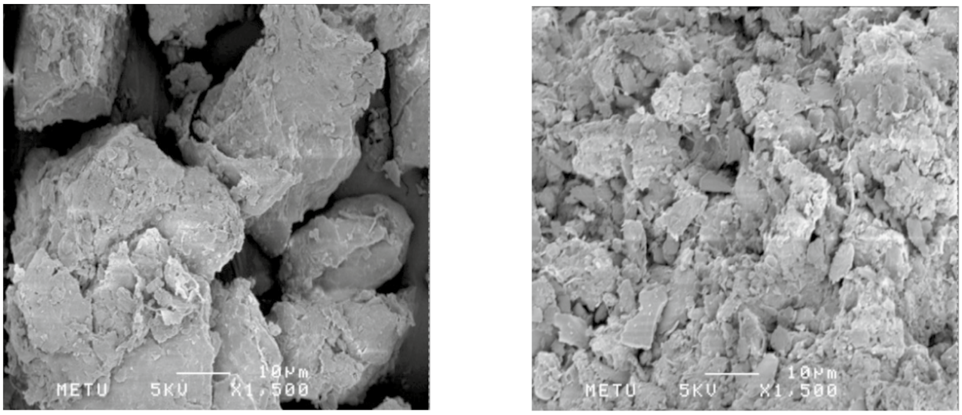

Sample-1 (<Rawand clean >)

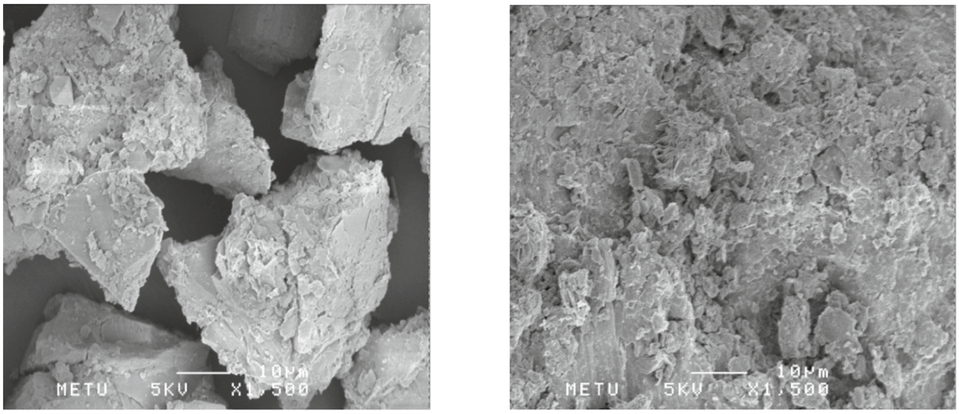

Sample-2 (< Raw and clean >)

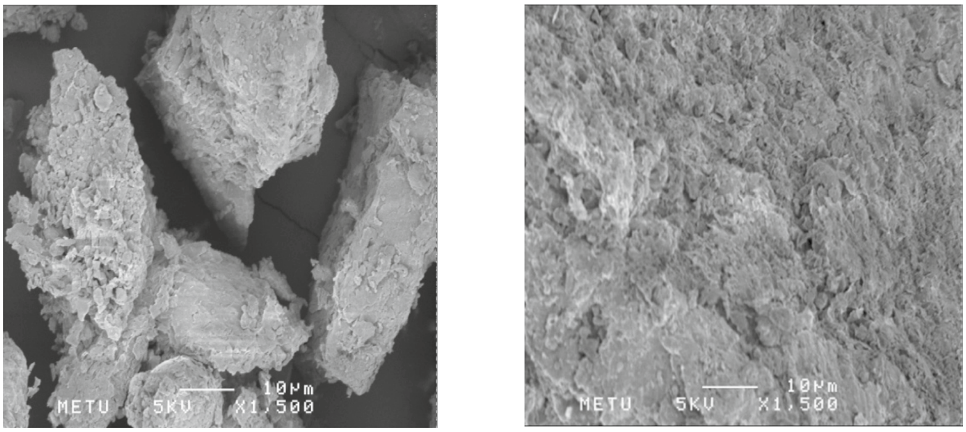

Sample-3 (< Raw and clean >)

particles. This pattern is consistent across all three samples and indicates a significant presence of inorganic contaminants such as clay minerals, carbonates, and siliceous matter. The fine particulates also contribute to a rough and irregular surface morphology, which is characteristic of unprocessed lignite.

In the cleaned samples, the SEM images demonstrate a substantial reduction in the abundance of fine and ultra-fine particulates. The coarser particles appear significantly less contaminated, with smoother surfaces and minimal particulate clustering in void spaces. This indicates the effectiveness of the cleaning process in removing ash-forming mineral matter.

The cleaned samples exhibit a more uniform texture, suggesting improved structural integrity and reduced impurity levels.

The transformation from raw to cleaned samples is clearly visible across all three samples. In raw samples, the extensive presence of fine particulates is indicative of the high ash and mineral content typical of untreated lignite. Conversely, the cleaned samples show a marked decrease in these particulates, aligning with the anticipated outcomes of the cleaning process. The reduced contamination in the cleaned samples likely contributes to improved combustion characteristics, as fewer inorganic impurities enhance thermal reactivity and reduce ash production. The significant reduction in fine particulates and the smoother surfaces observed in the cleaned samples suggest a notable decrease in ash-forming components such as silicates, carbonates, and clays. These improvements are critical for enhancing fuel quality, as lower ash content translates to increased energy efficiency and reduced environmental impact during combustion.

Reactivity and combustion index of lignite samples

To evaluate the ignition and combustion characteristics of lignite samples, combustion parameters such as the combustion index (S) and reactivity (R) were calculated for both raw and cleaned samples (Table 3). These parameters provide quantitative insights into the thermal behavior of lignite, specifically its ignition stability and reaction dynamics under combustion conditions. The equations used to compute the combustion index and reactivity are as follows:

$$S = R_{max} x\ R_a / T_i^2 x\ T_b \tag{1}$$

$$R = \left(-1/W_o\right) x\ (dW/dt) \tag{2}$$

The combustion characteristics of both raw and cleaned lignite samples were assessed based on ignition temperature, maximum mass loss, and burnout temperature. From the point view of ignition temperature, the cleaned samples exhibit lower ignition temperatures compared to raw samples, suggesting that the removal of mineral matter during cleaning reduces the thermal barrier to combustion initiation. Cleaned samples also demonstrate higher maximum mass loss rates, indicative of improved fuel reactivity and enhanced energy release. Also, the burnout temperatures of cleaned samples are slightly lower than those of raw samples, reflecting faster combustion completion.

The combustion index is a critical parameter for assessing the stability and efficiency of lignite combustion under varying conditions. Cleaned samples consistently show higher combustion index values compared to raw samples. This improvement is attributed to the reduction in mineral matter content, which decreases ash formation and facilitates more stable and efficient combustion.

On the other hand, reactivity is a measure of the rate at which the lignite reacts during combustion at specific conversion rates. Cleaned samples exhibit significantly higher reactivity values, underscoring the enhanced combustion dynamics achieved through the removal of mineral impurities. The increased reactivity is likely due to the exposure of more reactive organic components following the elimination of ash-forming minerals. Furthermore, the lower ignition and burnout temperatures observed in cleaned samples indicate a reduced energy requirement for initiating and sustaining combustion. This can lead to higher thermal efficiency and lower greenhouse gas emissions during fuel utilization.

DSC analysis

Differential scanning calorimeter (DSC) analysis provides critical insights into the thermal behavior of both raw and cleaned lignite samples. The DSC curves for samples 1, 2, and 3 (Fig. 3) highlight significant differences in heat flow and reaction characteristics between the raw and cleaned lignites, offering a deeper understanding of the effects of the cleaning process on combustion behavior.

In the low-temperature region, all lignite samples exhibit a small loss of pyrolysis water resulting from the decomposition of phenolic structures. Additionally, carbon oxides are released from carboxylic and carbonyl groups. These observations are consistent across raw and cleaned samples, indicating minimal impact of cleaning on this initial dehydration phase.

Primary carbonization begins at approximately 210 °C and is characterized by the release of various volatile components, including carbon dioxide, hydrogen, methane, lower aliphatics, carbon monoxide, and alkyl aromatics. In this region, the heat flow rates for cleaned samples are consistently lower, ranging from 5275 to 9480 J g^{-1}, compared to 6250 to 14,210 J g^{-1} for raw samples. This reduction reflects the removal of mineral matter, which typically contributes to non-combustible thermal reactions in raw samples. Also, cleaned samples show elevated peak temperatures within the primary carbonization region, suggesting that the organic matrix becomes more thermally stable following the removal of inorganic impurities. In this region, cleaned samples exhibit narrowed carbonization intervals, indicating a more concentrated and efficient release of volatiles. This suggests improved combustion efficiency due to the cleaner organic content of the samples. Certain cleaned lignite samples exhibit a secondary carbonization region not observed in raw samples. This phenomenon may be attributed to structural changes induced by the cleaning process, which could enhance the decomposition of residual carbonaceous material.

The observed decrease in heat flow values across cleaned samples underscores the efficiency of the cleaning process in removing inorganic components such as clays, siliceous matter, and carbonates. On the other hand, the increased peak

Fig. 3 DSC figures of raw and clean lignite samples 1, 2, and 3

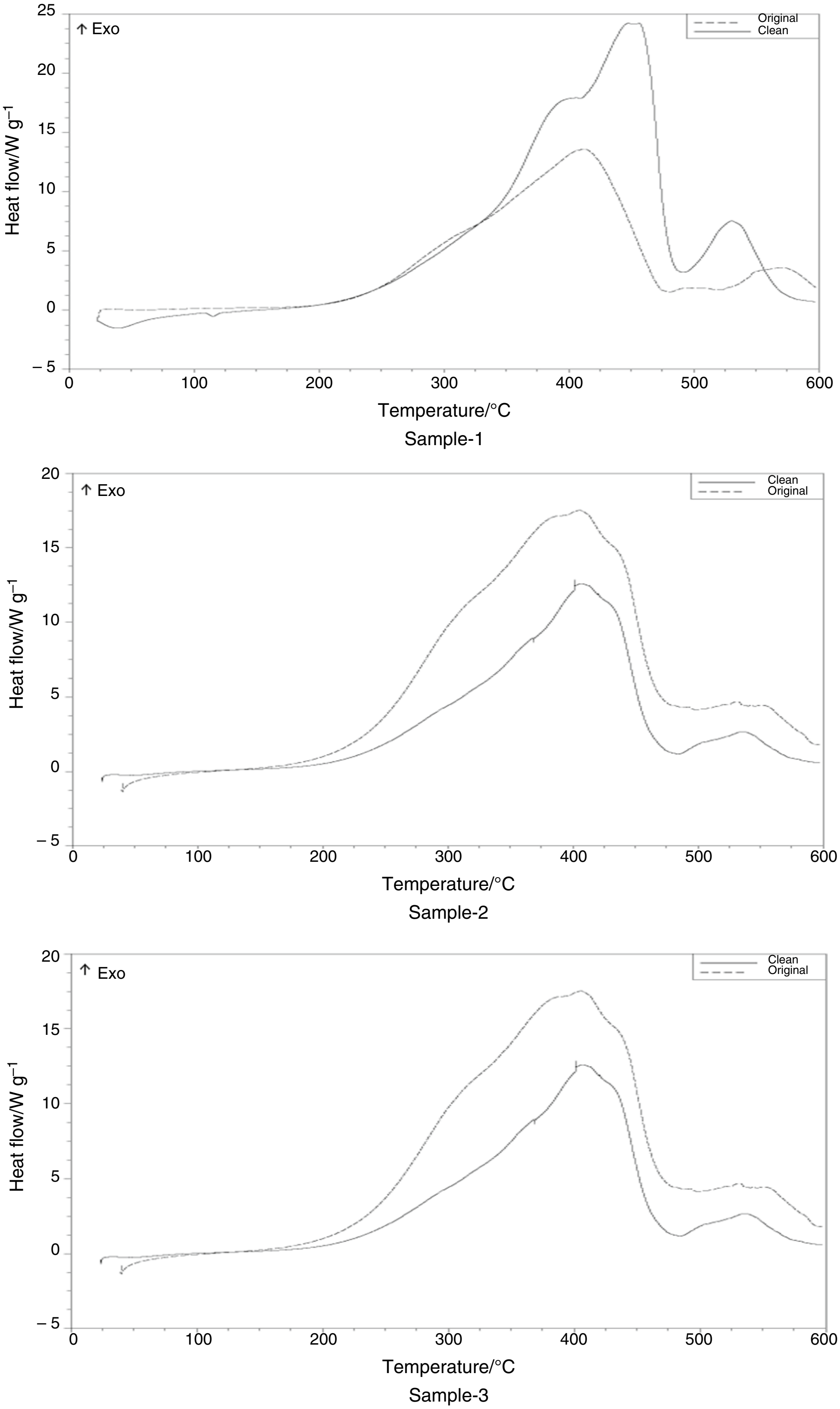

temperatures and narrowed carbonization intervals in cleaned samples suggest improved reactivity and energy release, making the fuel more efficient for combustion applications (Table 4).

PDSC analysis

The effect of pressure on the combustion characteristics of raw and cleaned lignite samples (samples 1, 2, and 3)

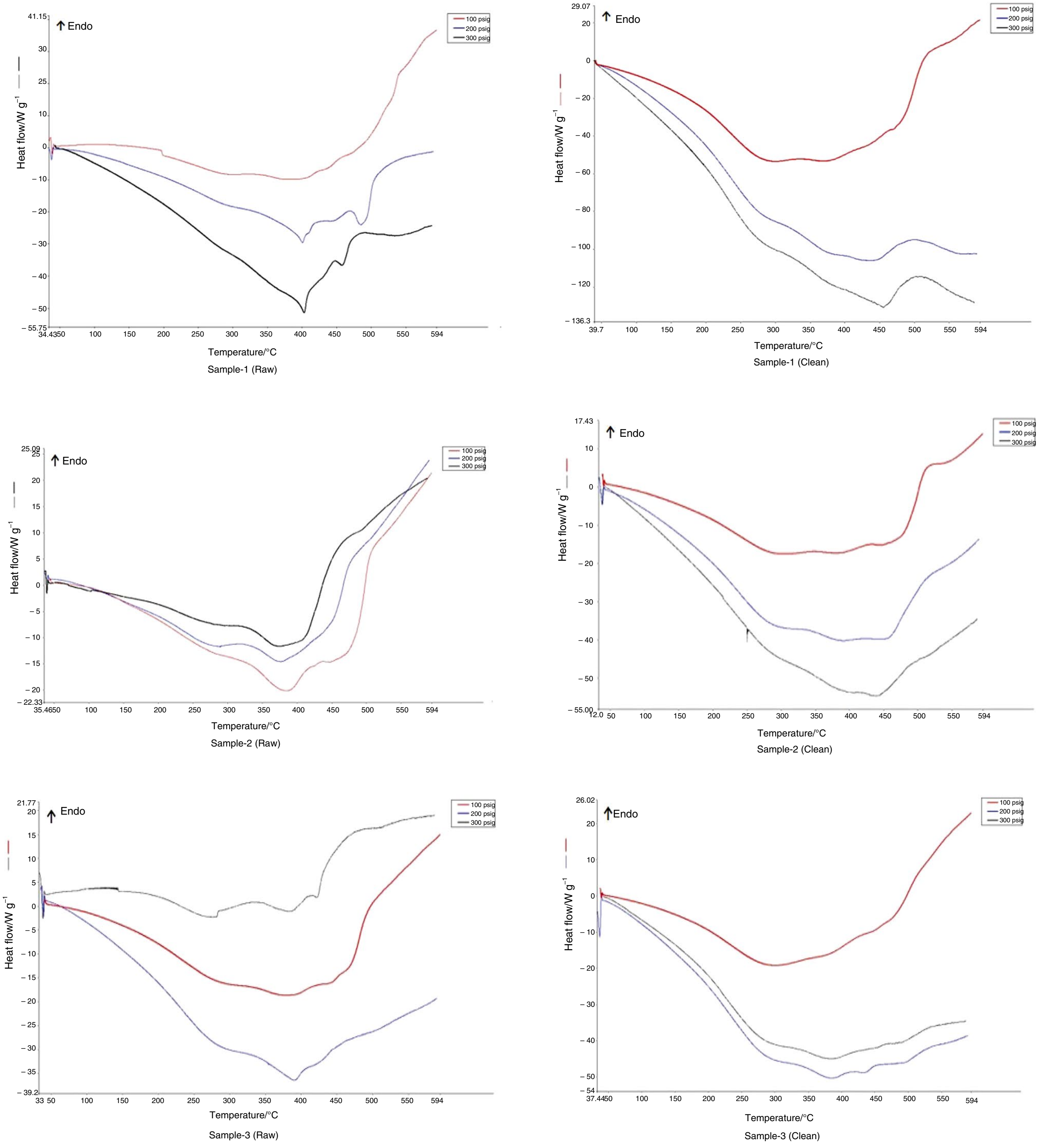

Fig. 4 PDSC figures of raw and clean lignite samples 1, 2, and 3

was thoroughly examined through pressurized differential scanning calorimeter (PDSC) experiments. These experiments were conducted at pressures of 100, 200, and 300 psig (Fig. 4). An increase in peak temperatures with escalating pressure is observed in raw samples. This indicates enhanced thermal stability and a delay in the maximum energy release due to the compacting effect of higher pressure, which may restrict oxygen diffusion and slow the reaction rates. In contrast, the peak temperatures in cleaned samples are consistently lower than those in raw samples due to the removal of mineral matter and impurities that inhibit thermal reactions.

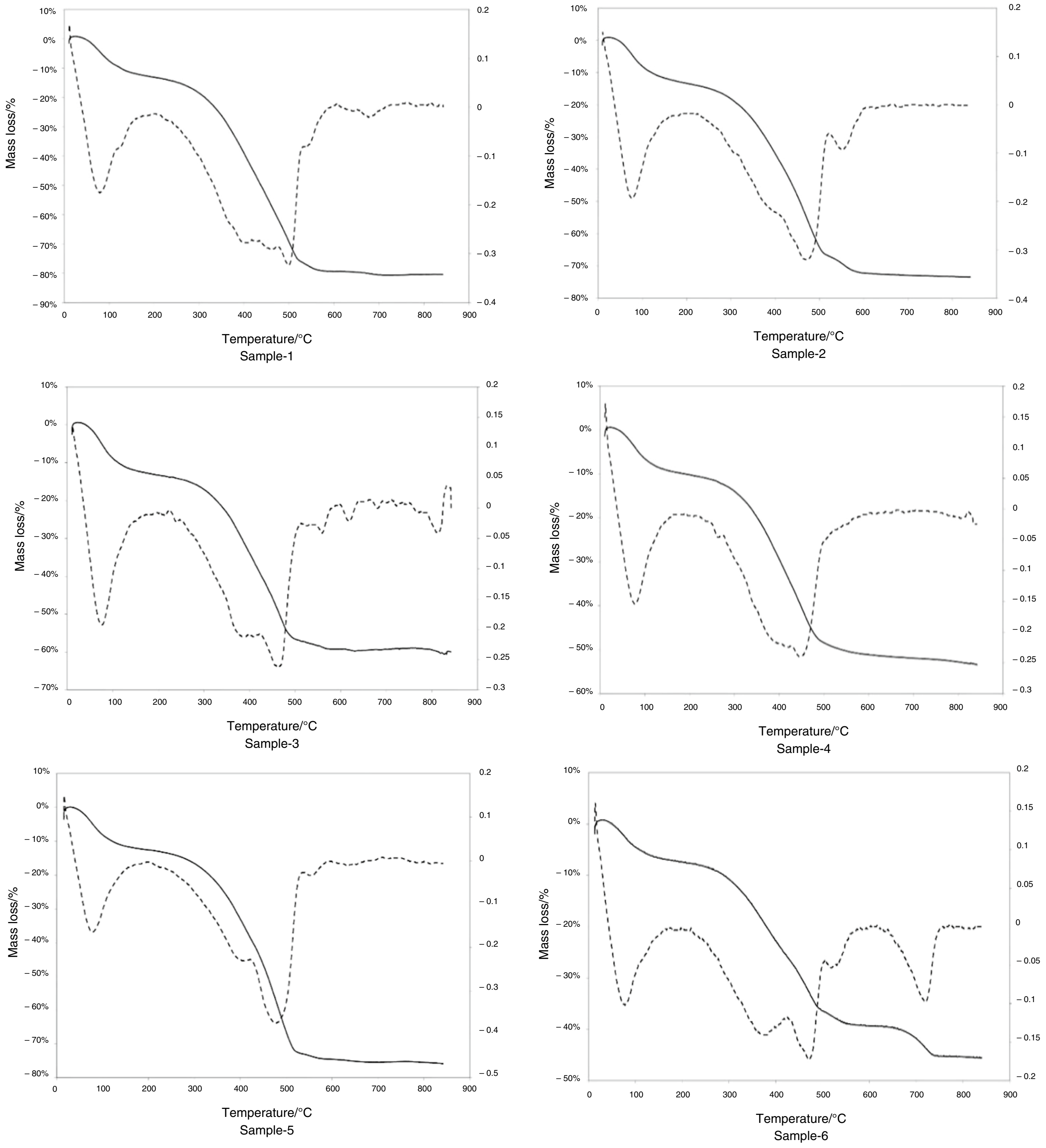

Fig. 5 TG–DTG figures of raw lignite samples

The cleaner organic matrix in these samples facilitates earlier and more efficient combustion.

The analysis of heat flow rate values reveals a pressure-dependent decline as the pressure increases from 100 to 300 psig (Table 5). This consistent reduction suggests that elevated pressures suppress the overall energy release rate during combustion. Several factors may contribute to this behavior such as kinetic modulation, reduced volatile escape, and enhanced thermal stability. The contrasting behaviors of raw and cleaned samples under pressure underscore the significant influence of the cleaning process on

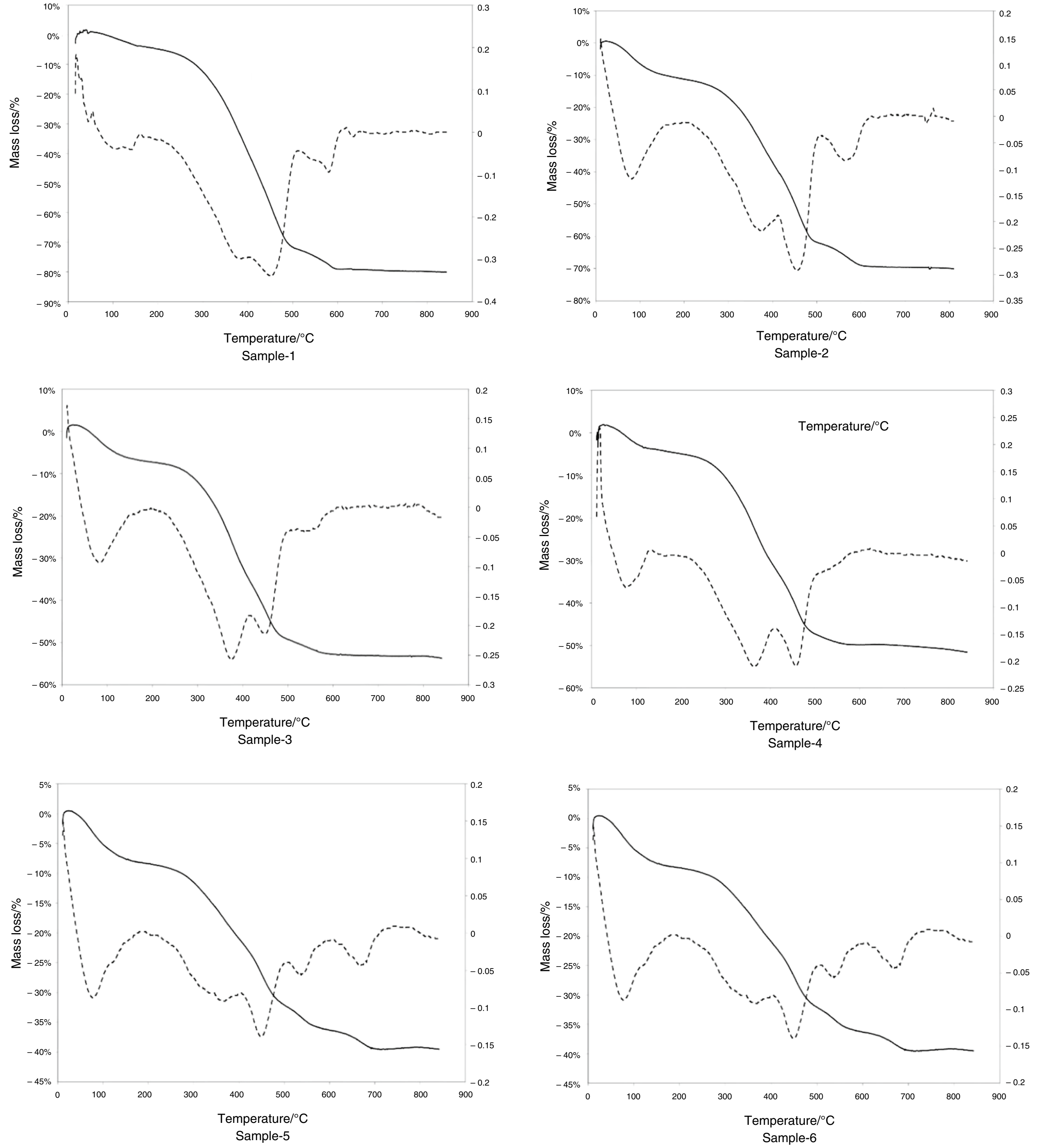

Fig. 6 TG–DTG figures of clean lignite samples

lignite combustion characteristics. The lower peak temperatures and reduced heat flow rates in cleaned samples suggest that removing mineral impurities enhances the accessibility and reactivity of the organic components, resulting in more efficient combustion.

TG–DTG analysis

Simultaneous thermogravimetry and differential thermal analysis coupled with multiple ion detection (TG–DTG–MID) provide valuable insights into the

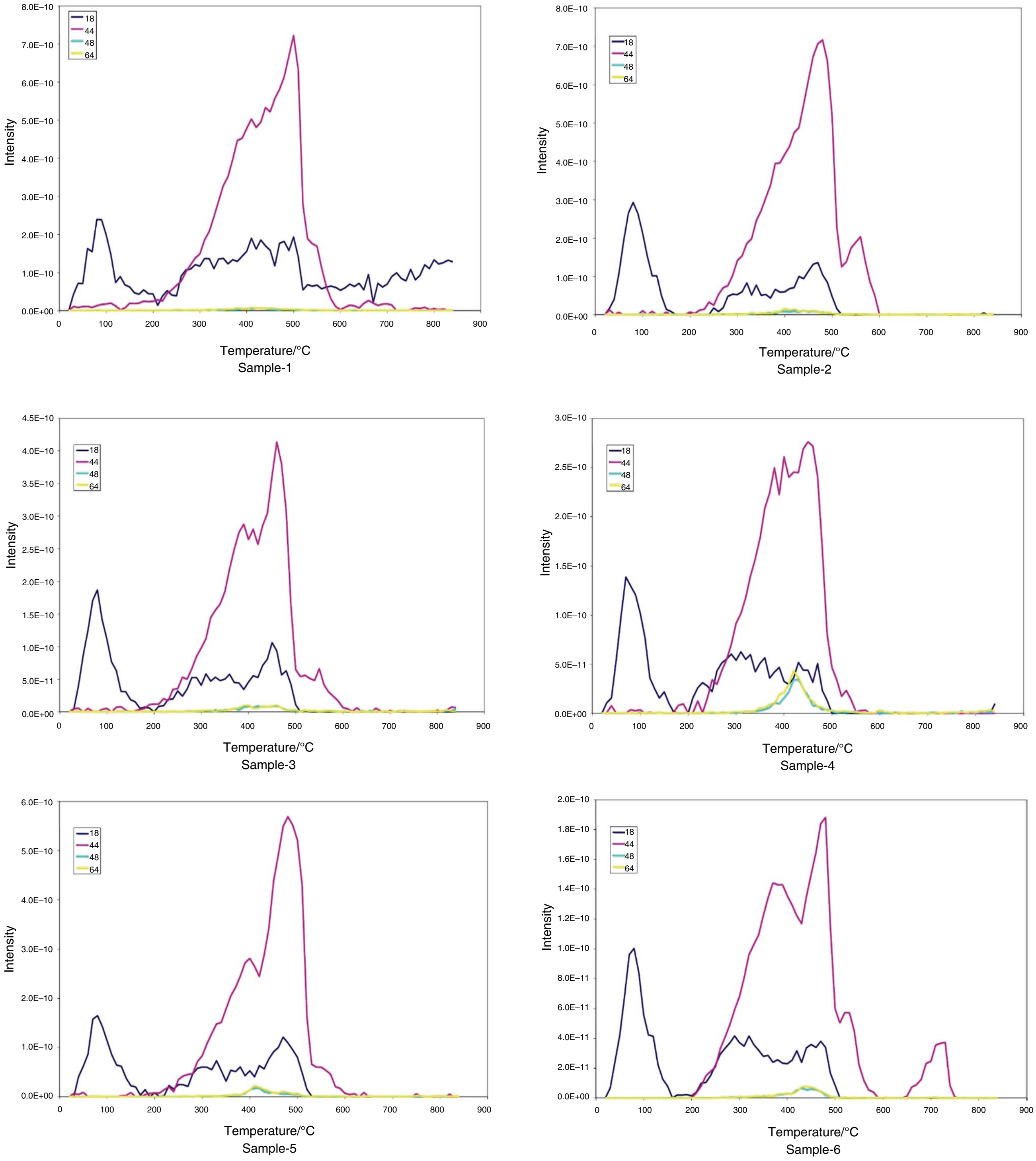

Fig. 7 TG–MID figures of raw lignite samples

combustion behavior of lignite samples. The TG–DTG curves reveal three distinct reaction regions that play critical roles in understanding the thermal and combustion properties of lignite. The initial mass loss due to moisture evaporation occurred at low temperatures. The primary region of mass loss is characterized by the release of volatile components and the combustion of organic carbon. This phase is critical for lignite combustion kinetics as it governs the release of energy-rich volatiles and the oxidation of carbon. The cleaned lignite samples exhibit elevated end temperatures in this region compared to their raw counterparts. Also, clean samples consistently show lower peak

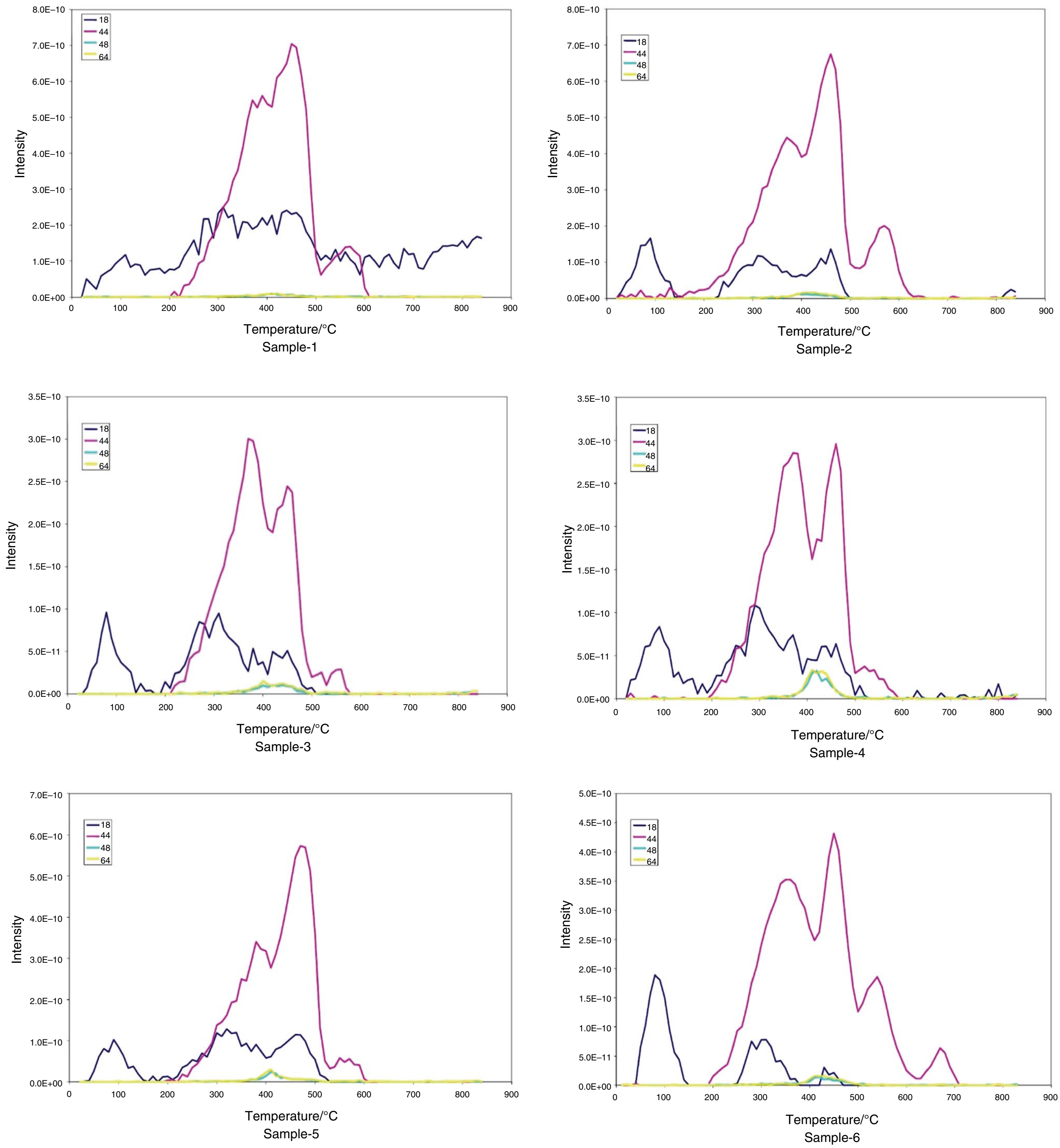

Fig. 8 TG–MID figures of clean lignite samples

temperatures than raw samples, reflecting the increased reactivity and reduced thermal resistance of the organic components after cleaning. The final reaction region is characterized by the decomposition of mineral matter, contributing to the ash content of the lignite. In cleaned samples, a notable reduction in this region's burnout temperature is observed, indicating more efficient combustion (Table 6). This improvement can be attributed to the removal of inert mineral components during the cleaning process, which otherwise hinder complete oxidation and prolong burnout times. (Figs. 5–6).

The primary region of mass loss in cleaned samples demonstrates increased efficiency, with higher percentages of volatiles and carbon contributing to energy release. The

Table 1 Properties of raw lignite samples

Sample	Heat value/kcal kg^{-1}	Moisture/%	Ash/%	Volatile/%	C/%	S/%	Gas/%	Density/g cm^{-3}	R$_{max}$/%
Sample 1	2310	37.32	21.26	24.74	16.68	2.91	62.06	1.35	0.443
Sample 2	2255	39.77	19.84	22.87	17.52	2.36	62.64	1.42	0.452
Sample 3	2115	31.25	29.14	20.42	18.14	2.81	52.06	1.43	0.448
Sample 4	2297	30.65	28.50	25.14	15.71	2.66	55.79	1.42	0.443
Sample 5	2395	31.84	25.42	22.91	19.83	3.24	54.75	1.43	0.452
Sample 6	2341	30.87	27.76	24.80	16.57	3.65	55.67	1.41	0.502

Table 2 Maceral and mineral matter content of raw lignite samples

Sample	Huminite vol. %/mmf						Total huminite	Liptinite vol. %/mmf					Toplam liptinite
	Tex	Texu	Eu	Den	Att	Gel	(%)	Sp	Cut	Lip	Alg	Res	(%)
Sample 1	–	3	5	5	1	62	76	2	2	–	2	–	6
Sample 2	–	–	3	7	2	54	66	2	1	–	2	2	7
Sample 3	–	3	7	4	–	51	65	2	1	–	–	–	3
Sample 4	–	5	17	9	3	40	74	1	1	1	–	–	3
Sample 5	2	6	7	3	–	55	73	3	–	1	–	–	4
Sample 6	–	–	4	4	1	46	55	2	–	1	–	–	3

Sample	Inertinite vol. %/mmf				Total inertinite	Mineral matter/%	
	Mac	Fus	Scle	In	(%)	Pyr	MM
Sample 1	3	1	–	–	4	5	09
Sample 2	2	1	–	–	3	4	20
Sample 3	2	–	1	–	3	6	23
Sample 4	2	1	–	–	3	5	15
Sample 5	2	–	–	1	3	7	13
Sample 6	2	–	–	1	3	7	32

mmf mineral matter-free basis; *Tex* textinite; *Texu* textoulminite; *Eu* eu-ulminite; *Den* densinite; *Att* attrinite; *Gel* gelinite; *Sp* sporinite; *Cut* cutinite; *Lip* liptodetrinite; *Alg* alginite; *Res* resinite; *Mac* macrinite; *Fus* fusinite; *Scle* sclerotinia; *In* inertodetrinite; *Pyr* pyrite; *MM* mineral matter other than pyrite (clay, inorganic matter)

significant reduction in ash-forming mineral content further supports the improved combustion characteristics of cleaned lignite.

TG–DTG–MID analysis

The TG–DTG–MID experiments provide a nuanced understanding of lignite combustion dynamics by monitoring the evolution of critical gaseous compounds, including water (m/z 18), carbon dioxide (m/z 44), and sulfur dioxide (m/z 64), at different temperatures and intensities (Figs. 7–8). These findings (Table 7) underscore the complex interplay between combustion environments and the material composition of both raw and cleaned lignite samples.

An examination of raw lignite sample 1 reveals a degradation occurring in two distinct steps, collectively accounting for up to 82% of the sample mass. Initially, a 14% loss is

Table 3 Reactivity and combustion–ignition index of raw and clean lignite samples

Sample	Combustion Index—S/ mass %$^{-1}$ min^{-1} °C	Reactivity—R/ min^{-1}
Raw 1	6.97	0.32
Clean 1	*7.63*	*0.34*
Raw 2	3.64	0.29
Clean 2	*5.50*	*0.32*
Raw 3	4.30	0.26
Clean 3	*4.55*	*0.28*
Raw 4	3.73	0.21
Clean 4	*3.81*	*0.24*
Raw 5	4.07	0.37
Clean 5	*9.84*	*0.43*
Raw 6	1.15	0.14
Clean 6	*1.18*	*0.18*

Table 4 DSC results of raw and clean lignite samples

Sample	Pyrolysis Water Region/°C	Primary Carb. Region/°C	Peak Temp./°C	Heat Flow Rate/J g-1
Raw 1	25–110	225–496	412	14,210
Clean 1	*25–110*	*195–490; 490–589*	*447; 531*	*8950*
Raw 2	25–110	215–520	418	10,095
Clean 2	*25–110*	*200–490; 490–596*	*439; 536*	*8295*
Raw 3	25–110	210–488	383	11,245
Clean 3	*25–110*	*195–478*	*397*	*9480*
Raw 4	25–110	210–470	365	12,080
Clean 4	*25–110*	*185–467*	*395*	*7905*
Raw 5	25–110	210–510	385	6460
Clean 5	*25–110*	*203–487*	*445*	*6280*
Raw 6	25–110	215–510	354	6250
Clean 6	*25–110*	*195–507; 507–575*	*398; 530*	*5275*

attributed to the expulsion of moisture content, succeeded by the combustion of the sample. Mass spectral investigations during these stages unveil the sequential evolution of H_2O, followed by the emergence of CO_2 and SO_2, where the presence of CO_2 and H_2O denotes hydrocarbon combustion, while SO_2 arises from the combustion of sulfur-containing components. Furthermore, a distinctive peak at 570 °C delineates a separate degradation step, constituting approximately 6% of the sample mass, thus emphasizing the discernible impact of the cleaning process on the combustion characteristics.

Table 5 PDSC results of raw and clean lignite samples

Sample	Primary Carb./°C	Peak Temp./°C	Heat Flow Rate/J gr-1
Raw 1 (100 psig)	220–475	394	20,125
Raw 1 (200 psig)	220–475	400	15,879
Raw 1 (300 psig)	220–475	404	13,432
Clean 1 (100 psig)	*215–480*	*374*	*22,275*
Clean 1 (200 psig)	*215–480*	*373*	*21,175*
Clean 1 (300 psig)	*215–490*	*381*	*19,258*
Raw 2 (100 psig)	215–490	380	20,520
Raw 2 (200 psig)	215–490	389	17,986
Raw 2 (300 psig)	215–490	401	15,387
Clean 2 (100 psig)	*215–490*	*374*	*25,157*
Clean 2 (200 psig)	*215–490*	*383*	*23,655*
Clean 2 (300 psig)	*215–490*	*396*	*21,752*
Raw 3 (100 psig)	215–480	386	16,070
Raw 3 (200 psig)	215–480	389	13,584
Raw 3 (300 psig)	215–480	391	11,244
Clean 3 (100 psig)	*215–480*	*290*	*16,750*
Clean 3 (200 psig)	*215–480*	*294*	*15,372*
Clean 3 (300 psig)	*215–480*	*295*	*15,231*

Similarly, raw lignite sample 2 exhibits a three-step degradation process, leading to the degradation of 74% of the sample mass, with the initial step accounting for 14% due to moisture loss, followed by subsequent steps attributed to sample combustion. Conversely, clean lignite sample 2 undergoes a four-stage degradation, resulting in the degradation of 70% of the sample mass. In this case, the first step (12%) is associated with moisture loss, while the subsequent steps involve sample combustion. The notable disparities in the evolution curves, particularly evident in the shift in maxima and the separation of steps, vividly illustrate the profound influence of the cleaning process on the combustion characteristics.

This analytical framework extends to raw lignite sample 3, characterized by a two-step degradation leading to the degradation of 60% of the sample mass, with its clean counterpart undergoing a three-step degradation, resulting in the degradation of 55% of the sample mass. Mass spectral investigations unveil the evolution of water during the initial steps, followed by the evolution of CO_2 and SO_2 during the subsequent burning stages. The cleaning process induces alterations in the evolution maxima, thereby emphasizing the nuanced variations introduced by the cleaning procedure.

Continuing the examination, raw lignite sample 4 experiences a two-step degradation, culminating in the degradation of 53% of the sample mass, whereas its clean counterpart undergoes a three-step degradation to the same percentage. The mass spectra exhibit the evolution of water during the initial step, followed by the evolution of CO_2 and SO_2 during the subsequent burning stages. Evidently, the influence of the cleaning process is discernible in the high-temperature peak and the shift in evolution maxima.

Raw lignite sample 5, exhibiting a four-step degradation of 75%, and its clean variant, displaying a four-step degradation of 84%, offer further instances of moisture

Table 6 TG–DTG analysis of raw and clean lignite samples

Sample	Evaporation Region/°C	Primary Carbon. Region/°C	Peak/Burnout Temp./°C	Mass Loss /% *-Primary Carbonization Region-*	Total Sample Left/%
Raw 1	30–200	200–540	502/705	66.1	19.7
Clean 1	*30–180*	*180–517*	*456/670*	*61.1*	*19.1*
Raw 2	25–205	205–525	475/700	56.1	28.1
Clean 2	*25–200*	*200–512*	*460/665*	*51.3*	*27.8*
Raw 3	25–215	215–542	476/680	45.3	39.1
Clean 3	*25–200*	*200–535*	*453/620*	*42.1*	*43.4*
Raw 4	30–195	195–550	460/700	42.7	43.6
Clean 4	*30–180*	*180–518*	*454/630*	*44.1*	*48.2*
Raw 5	35–205	205–548	482/690	61.1	25.3
Clean 5	*35–200*	*200–542*	*475/630*	*68.4*	*58.3*
Raw 6	30–200	200–512	490/715	31.2	54.1
Clean 6	*25–195*	*195–507*	*453/680*	*27.6*	*56.7*

loss followed by combustion. The mass spectra delineate the evolution of H_2O, CO_2, and SO_2 during these stages, with the cleaning process exerting a noticeable influence on the evolution maxima.

Lastly, raw lignite sample 6 manifests a five-step degradation, accounting for 46% of the sample mass, while clean lignite sample 6 undergoes a five-step degradation, resulting in the degradation of 40% of the sample mass. The distinctive steps encompass the evolution of moisture loss and subsequent combustion stages, accompanied by H_2O, CO_2, and SO_2. Notably, the final degradation step above 600 °C is associated with the combustion of elemental carbon, possibly adopting a graphite-like structure. The cleaning process introduces shifts in evolution maxima and influences the quantity of evolved H_2O, CO_2, and SO_2.

As a whole, it was observed that the cleaning consistently alters the degradation pathways, introducing additional steps or modifying the progression of combustion stages. Shifts in temperature maxima for key reactions indicate enhanced reactivity and efficiency due to the removal of inert mineral matter. The evolution of H_2O (m/z 18), CO_2 (m/z 44), and SO_2 (m/z 64) is markedly influenced by cleaning, with cleaner samples showing reduced sulfur emissions and enhanced hydrocarbon combustion. Higher peak temperatures in raw samples indicate a delay in combustion due to the thermal resistance of mineral matter. Clean samples exhibit lower peak temperatures and narrower temperature intervals, reflecting improved thermal stability. Finally, the cleaning process generally reduces the overall mass loss percentage due to the removal of mineral matter, which contributes minimally to energy generation but significantly to ash formation.

Table 7 TG–DTG–MID results of raw and clean lignite samples

Sample	H_2O Peak Temp./°C	CO_2 Peak Temp./°C	SO_2 Peak Temp./°C
Raw 1	80, 410, 500	410, 440, 500, 550	410
Clean 1	*110, 280, 310, 430*	*370, 390, 450, 570*	*420*
Raw 2	80, 330, 470	390, 480, 560	400, 550
Clean 2	*90, 310, 460*	*370, 460, 570*	*420, 570*
Raw 3	80, 310, 450	390, 460, 550	400,460
Clean 3	*80, 310, 450*	*370, 460, 560*	*400, 440*
Raw 4	70,310, 430	380, 400, 450	420, 600
Clean 4	*90, 290, 370*	*370, 460, 540*	*410, 430*
Raw 5	80, 330, 470	410, 480, 550	410, 470, 500
Clean 5	*90, 320, 470*	*380, 470, 550*	*410, 490*
Raw 6	80, 320, 470	370, 480, 530, 770	400, 440
Clean 6	*80, 300, 430*	*350, 450, 540, 670*	*340, 430*

Conclusions

This investigation employs a comprehensive suite of analytical techniques, including thermogravimetry–multiple ion detection (TG–DTG–MID), differential scanning calorimeter (DSC), and pressurized differential scanning calorimeter (PDSC), to identify the combustion characteristics of both raw and cleaned lignite samples. The key findings from these analyses are summarized as follows:

DSC analysis reveals that cleaning lignite has a profound impact on its thermal behavior, improving combustion efficiency by reducing heat flow requirements, narrowing carbonization intervals, and increasing thermal stability. These findings validate the importance of beneficiation processes in optimizing lignite for energy applications.

PDSC experiments reveal that pressure plays a crucial role in influencing lignite combustion, with cleaner samples exhibiting more efficient and predictable behavior across varying pressure levels. These results emphasize the importance of the cleaning process in enhancing lignite's suitability for high-pressure combustion applications.

The results from TG–DTG analysis demonstrate the transformative effects of the cleaning process on lignite combustion characteristics. The reduced burnout temperature, enhanced reactivity, and higher energy release from cleaned samples emphasize the importance of beneficiation in optimizing lignite for energy applications.

The TG–DTG–MID analysis provides critical insights for optimizing lignite processing and utilization, with potential applications in industrial combustion systems aiming for higher energy efficiency and lower environmental impact. Further investigations integrating emission analysis and kinetic modeling could offer deeper insights into these transformations.

Acknowledgements The author extends sincere gratitude for the financial support provided by The Scientific and Technological Research Council of Türkiye (TÜBİTAK-MAG 107-T-305) and the partial support provided by the Ministry of Science and Higher Education of the Russian Federation under agreement No. 075-15-2022-299. This funding has been pivotal in enabling the establishment of a state-of-the-art research center focused on advancing the efficient exploration and development of global liquid hydrocarbon reserves.

Author contribution All authors contributed to the discussion of the results, revised the manuscript critically for important intellectual content, and approved the final version of the manuscript.

Funding Open access funding provided by the Scientific and Technological Research Council of Türkiye (TÜBİTAK).

Declarations

Conflict of interest The authors declare that there is no conflict of interest regarding the publication of this paper.

References

1. Smith SE, Neavel RC, Hippo EJ, Miller RN. DTGA combustion of coals in the Exxon coal library. Fuel. 1981;60(6):458–62.
2. Kok MV. An investigation into the combustion curves of lignites. J Therm Anal Calorim. 2007;2001(64–3):1319–23.
3. Morgan PA, Robertson SD. Combustion studies by thermogravimetric analysis: coal oxidation. Fuel. 1986;65–11:1546–51.
4. Song Z, Huang X, Luo M, Gong J, Pan X. Experimental study on the diffusion-kinetics interaction in heterogeneous reaction of coal. J Therm Anal Calorim. 2017;129:1625–37.
5. Liu L, He D, Xu L, Yang H, Wang Q. Study of the combustion of Shuangya mountain coal by thermogravimetry. J Therm Anal Calorim. 1999;58–2:447–53.
6. Wu D, Huang X, Norman F, Verplaetsen F, Berghmans J, Bulck E. Experimental investigation on the self-ignition behavior of coal dust accumulations in oxy-fuel combustion system. Fuel. 2015;160:245–54.
7. Iordanidis A, Georgakopoulos A, Markova K, Fournaraki A. Application of TG-DTA to studying Amynteon lignites. Thermochim Acta. 2001;371–1:137–41.
8. Kok MV. An investigation into the thermal behavior of coals. Energy Sour. 2002;24–10:899–906.
9. Alonso MIG, Borrego AG, Alvarez D, Kalkreut W, Menendez R. Physico-chemical transformations of coal particles during pyrolysis and combustion. Fuel. 2001;83–13:1857–70.
10. Jayaweera SA, Moss JM, Thwaites MW. The effect of particle size on the Weardale coal. Thermochim Acta. 1989;152–1:147–50.
11. Sarwar A, Nasiruddin KM, Fizza K. Kinetic studies of pyrolysis and combustion of Thar coal by thermogravimetry and chemometric data analysis. J Therm Anal Calorim. 2012;109:97–103.
12. Mohalik NK, Panigrahi DC, Singh VK. Application of thermal analysis techniques to assess proneness of coal to spontaneous heating. J Therm Anal Calorim. 2009;98:507–19.
13. Kandasamy J, Kok MV, Gokalp I. Combustion mechanism and model-free kinetics of different origin coal samples: thermal analysis approach. Energy. 2020;204:117905.
14. Li Q, Zhao CC, Wu X, Li Y. Comparison of pulverized coal combustion in air and O_2/CO_2 mixtures by thermo-gravimetric analysis. J Anal Appl Pyrol. 2009;2009(85):521–8.
15. Wang C, Du Y, Che D. Reactivities of coals and synthetic model coal under oxy-fuel conditions. Thermochim Acta. 2013;553:8–15.
16. Ozbas KE, Hicyilmaz C, Kok MV, Bilgen S. Effect of the cleaning process on combustion characteristics of lignite. Fuel Proc Techn. 2002;64:211–20.
17. Erarslan C, Orgun Y. Mineralogical and geochemical characterization of the Saray and Pınarhisar coals, Northwest Thrace Basin. Turkey Int J Coal Geol. 2017;173:9–25.
18. Siyako M. Properties of sandstone in Thrace basin. Mineral Res Explor Inst Bull. 2006;132:63–73.